Transition dipole strength of eumelanin

J. J. Riesz,[1,*] J. B. Gilmore,[1] Ross H. McKenzie,[1] B. J. Powell,[1] M. R. Pederson,[2] and P. Meredith[1]
[1]*Condensed Matter Physics Group, Physics Department, University of Queensland, St. Lucia, Brisbane, QLD 4072, Australia*
[2]*Center for Computational Materials Science, U. S. Naval Research Laboratory, Washington D.C. 20375*
(Received 7 June 2007; published 15 August 2007)

We report the transition dipole strength of eumelanin (the principal human photoprotective pigment) in the ultraviolet and visible. We have used both theoretical (density functional) and experimental methods to show that eumelanin is not an unusually strong absorber amongst organic chromophores. This is somewhat surprising given its role as a photoprotectant, and suggests that the dark coloring *in vivo* (and *in vitro*) of the eumelanin pigment is a concentration effect. Furthermore, by observing the polymerization of a principle precursor (5,6-dihydroxyindole-2-carboxylic acid) into the full pigment, we observe that eumelanin exhibits a small amount (~20%) of hyperchromism (i.e., the reaction process enhances the light absorption ability of the resultant macromolecule relative to its monomeric precursor). These results have significant implications for our understanding of the photophysics of these important functional biomolecules. In particular, they appear to be consistent with the recently proposed chemical disorder secondary structure model of eumelanins.

DOI: 10.1103/PhysRevE.76.021915 PACS number(s): 87.15.−v

I. INTRODUCTION

Melanins are a class of biological pigments that function as photoprotectants in the skin, hair, and eyes of humans and many other species [1–3]. They are also found in the inner ear where they are important for hearing and in the brain stem where deficiencies have been related to Parkinson's disease [4,5]. The amount of melanin pigment in an individual's skin is very clearly linked to their risk of developing skin cancer, although it is not clear if melanin is always photoprotective: melanin has been shown to be photoreactive and capable of producing damaging reactive oxygen species and therefore could function as both photosensitizer and photoprotector. [6]. Of the different types of melanin found in human skin, eumelanin (a brown to black pigment) is the most common and most widely studied and is therefore the pigment of interest in this article.

Despite decades of research, several fundamental aspects of the physical properties of eumelanin remain unclear (for a recent review on the physics and chemistry of eumelanin, see Ref. [7]). This is due in part to a number of inherently challenging material properties such as insolubility, structural disorder, and broadband absorption (making spectroscopic analysis difficult) [8]. In particular, the supramolecular structure of eumelanin remains a source of uncertainty which significantly hampers attempts at theoretical and structural analysis. Eumelanin is known to be a macromolecule of 5,6-dihydroxyindole (DHI) and 5,6-dihydroxyindole-2-carboxylic acid (DHICA), but the manner in which these units combine (here referred to as the secondary structure in a nomenclature borrowed from proteins) is uncertain [9].

Eumelanin exhibits a broadband absorption spectrum that increases towards the UV (Fig. 1). This is unusual amongst organic chromophores which typically possess identifiable absorption peaks corresponding to transitions between distinct electronic energy levels (broadened by interactions with the solvent and/or environment). Eumelanin, however, has no distinct peaks within the UV and visible frequency range. Humic substances (decayed plant and animal matter) have similarly unusual optical properties [10–15]. It has been proposed that this somewhat unusual spectrum is caused by optical Mie and Rayleigh scattering [16]. However, it has recently been shown that scattering does not contribute substantially to the extinction coefficient of eumelanin [17]. For more than three decades melanins have been considered amorphous semiconductors [18–23]. This description was (and continues to be) motivated by the observation of threshold switching [24] and a pronounced UV-visible light photovoltaic response [25–27]. In this model the semiconductor electronic band structure provides a sufficient (but certainly not necessary) explanation for the observed broadband absorbance. More recently, the chemical disorder model has also provided a natural explanation for the optical properties of eumelanin [28]. In this model, the pigment is essentially an ensemble of chemically distinct oligomeric macromolecules each with an individual highest-occupied-molecular-orbital- (HOMO-) lowest-unoccupied-molecular-orbital (LUMO) gap energy and related transition dipole moment for the first excited state. A small number (of the order of 10) of these macromolecular species with inhomogeneously broadened excitation transitions could account for a smooth, monotonic absorption profile extending from the UVB to NIR (Fig. 1).

The work described in this article is motivated by a desire to probe the chemical disorder hypothesis and specifically investigate whether eumelanin as a pigment has an unusually high absorbance (relative to other organic and bio-organic chromophores) in the UV and visible. To the first order, if eumelanin were merely a disordered ensemble of chemically distinct macromolecules, one would expect the "system" to possess an integrated transition dipole moment similar to that of the sum of its individual parts. To this end, we have measured the extinction coefficients for a number of species, namely, synthetic eumelanin, DHICA (as a monomer and during its polymerization to eumelanin), tyrosine, and fluorescein (a strongly fluorescent, well-characterized dye, used

*riesz@physics.uq.edu.au

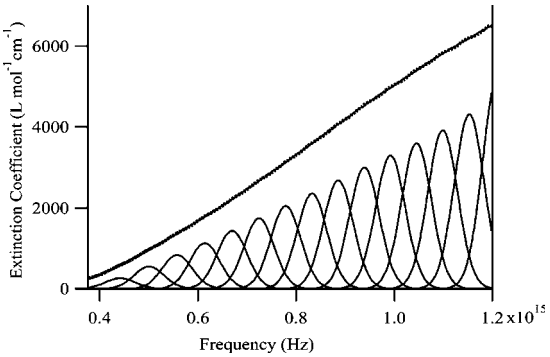

FIG. 1. The extinction coefficient of eumelanin vs frequency (solid) with multiple Gaussian fitting (dotted) (experimental spectrum as reported in Ref. [29]). The chemical disorder model suggests that the broadband absorption spectrum of eumelanin can be reproduced by the summation of multiple Gaussian spectra with widths typical of solvent broadening for organic chromophores [9]. In order for this model to be consistent with the observed data, those species absorbing at higher energies must have either a higher abundance or larger oscillator strengths to produce the monotonic increase in the absorption towards higher energies.

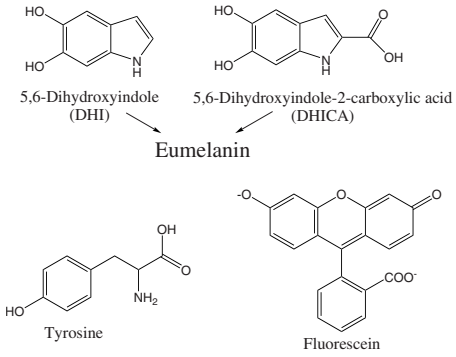

FIG. 2. The chemical structures of molecules relevant to this study. DHI and DHICA are the basic monomeric building blocks of the eumelanin macromolecule, whereas tyrosine is an earlier precursor. Fluorescein is a commonly used organic dye and quantum yield standard.

here as a standard for comparison). Chemical structures of these molecules are shown in Fig. 2. From these spectra we have extracted dipole strengths, transition dipole moments, and oscillator strengths. In addition, we have measured photoluminescence spectra for tyrosine, fluorescein, and eumelanin and used these to determine radiative rates and lifetimes. These have been compared to literature values for verification of our methods. For a final comparison, transition energies and dipole strengths of these compounds have been predicted from first principles via density functional theory.

II. THEORY

The extinction coefficient of a solution ϵ as a function of frequency ν can be determined from the experimentally measured absorbance (A, dimensionless) via

$$\epsilon(\nu) = \frac{A(\nu)}{lC}, \quad A(\nu) = -\log_{10}\left(\frac{I}{I_0}\right), \tag{1}$$

where l is the path length over which the absorbance occurs (the distanced light travels through the sample), I/I_0 is the fraction of light not absorbed in that path length, and C is the concentration of the solution. In these calculations it is important to be careful with units, since a variety are used both in the experimental and theoretical literatures. We will therefore be very explicit about the units used throughout this section. If the concentration in Eq. (1) is in moles per liter (mol/L) the extinction coefficient will be in the typically used units of L mol^{-1} cm^{-1}. The extinction coefficient is thus a concentration and path length independent measure of the optical attenuation of a material (although it may be affected by the choice of solvent).

The dipole strength of an electronic transition (D, in units of C^2 m^2) can be determined from an experimentally measured absorption spectrum via the following expression [30,31]:

$$D = \frac{3\epsilon_0 \hbar c}{\pi N_A} n \int_{\Delta\nu} \frac{\epsilon(\nu)}{\nu} d\nu, \tag{2}$$

where all constants are in SI units, $\epsilon(\nu)$ is the extinction coefficient expressed in m^2 mol^{-1}, $\Delta\nu$ is the frequency range over which the transition occurs, and n is the average refractive index of the solvent in a region of space around the chromophore of the order of an optical wavelength (we approximate this here by the refractive index of the bulk solvent). This calculation assumes that you can clearly identify and integrate over a single electronic transition (which is not always possible in an experimental spectrum). Note that 1 m^2 mol^{-1} = 10 L mol^{-1} cm^{-1}. D may be converted to the commonly used units of D^2 via 1 D^2 = 1.1127 $\times$ 10^{-59} C^2 m^2. From the dipole strength one may then determine the magnitude of the transition dipole moment $\mu_{ij} = e\langle j|\vec{r}|i\rangle$ between two states $|i\rangle$ and $|j\rangle$,

$$D = |\mu_{ij}|^2. \tag{3}$$

Note that for clarity we have suppressed the subscripts i and j on D and other parameters where they are understood. We can also determine the dimensionless oscillator strength f

$$f = \left(\frac{4\pi m_e \nu}{3e^2\hbar}\right) D, \tag{4}$$

where e and m_e are the charge and mass of an electron, respectively, ν is the frequency of the transition, and all values are in SI units (including D in C^2 m^2).

A. Radiative rates

The radiative rate of a material in a medium of index n is given by the Strickler-Berg relation [30]

$$A = \frac{1}{4\pi\epsilon_0} \frac{64\pi^4 n \langle \nu^{-3}\rangle^{-1}}{3hc^3} D, \tag{5}$$

where all quantities are in SI units (including D in C^2 m^2). A is the radiative rate in s^{-1} and the angular brackets indicate an average weighted by the emission spectrum

$$\langle \nu^{-3} \rangle^{-1} = \frac{\int f(\nu) d\nu}{\int \nu^{-3} f(\nu) d\nu}, \quad (6)$$

where $f(\nu)$ is the emission spectrum. A is also known as the Einstein coefficient of spontaneous emission [31]. The lifetime of the excited state (τ) is then given by

$$\tau = \frac{\Phi}{A}, \quad (7)$$

where Φ is the radiative quantum yield (the ratio of photons emitted to photons absorbed by a material) [32].

B. The effect of the solvent

The dipole strength of a chromophore in solution may be changed from the intrinsic dipole strength of the isolated chromophore (gas phase). To a good approximation, although different solvents will change the position and width of the absorption peaks (and hence the extinction coefficient), in the absence of specific solute-solvent interactions (such as hydrogen bonding or conformational changes) the change in dipole strength of the chromophore in solution depends only on the solvent refractive index [33,34]. This result can be obtained from "reaction-field-type" models [35], modeling the solvent as a bath of harmonic oscillators, for which sum rules can be obtained [36]. The dipole strengths obtained experimentally in this paper are therefore expected to differ from those of an isolated molecule, as calculated by NRLMOL. Corrections may be possible through a reaction-field-type calculation [33,37].

III. EXPERIMENTAL

A. Sample preparation

1. Eumelanin

Synthetic eumelanin powder was purchased from the Sigma Chemical, Co. (lot No. 60K1383, prepared by oxidation of tyrosine with hydrogen peroxide) and used without further purification. The powder was solubilized to form a 0.1% solution (by weight) in pH12 NaOH (the lowest pH at which the powder would solubilize properly, hence avoiding scattering effects [17]) and sonicated for approximately 15 min. to ensure complete solubilization. This stock solution was then diluted to concentrations (by weight) of 0.001, 0.0025, and 0.005 %. The integrated scattering was measured directly and found to be negligible [17]. The dipole strength was determined for each solution over the frequency range indicated in Table I and averaged to give the reported value.

2. DHICA

DHICA was synthesized as reported by Tran *et al.* [28]. It was solubilized in pH 9 NaOH at a 2 mM concentration. The absorbance was measured and scaled using a published value for the extinction coefficient at the 316 nm peak [38]. The oxidative polymerization of this solution was monitored by the extraction of aliquots at 0, 0.5, 1, 2, 4, 8, 12, 24, 51, and 74 h. For a more complete experimental method see Ref. [28].

TABLE I. Absorption parameters as defined in the theory section extracted from extinction coefficients in Fig. 3 (D: dipole strength, μ: transition dipole moment, f: oscillator strength). These are typically determined for a particular peak or transition, but this is not possible for a broadband spectrum such as that for eumelanin, hence the frequency ranges over which the integrations of experimental data were performed to determine the dipole strength and other parameters are as listed ($\Delta\nu$). Data in brackets are from Ref. [54] over the same frequency range for comparison. Discrepancies between these results and those found in literature may be attributed to difference in solvents (which can affect the dipole strength via second order effects) and uncertainty in concentration. Since the secondary structure of eumelanin is unknown it is necessary to determine these parameters in terms of N, the average number of monomers per oligomer (as described in the text). The dipole strength per monomer of eumelanin (37) is comparable to that of DHICA (31), much larger than that of tyrosine (1.6), and much smaller than that of fluorescein (140). This suggests that eumelanin is not an exceptionally strong absorber as might have been assumed due to its photoprotective biological role.

	D (Debye^2)	μ (Debye)	f (dimensionless)	$\Delta\nu$ (10^{15} Hz)
Tyrosine	1.6	1.3 [1.04]	0.027 [0.019]	0.375 to 1.2
Eumelanin	$37N$	$6.1\sqrt{N}$	$0.53N$	0.5 to 1.2
DHICA	31	5.6	0.46	0.5 to 1.2
Fluorescein	140	12 [7.0]	1.3 [0.46]	0.5 to 0.75

3. Tyrosine

D-Tyrosine (99%, batch 14424MA) was purchased from Aldrich and solublized in 1 M HCl to a concentration (by weight) of 0.0025%.

4. Fluorescein

Fluorescein is known to have various forms, but at the pH used in this study it exists in the dianionic form as shown in Fig. 2 [39]. Fluorescein (Aldrich, F2456–100G, Batch 09014PA, Dye content around 95%) was solubilized in 0.1 M NaOH solution and diluted to give five solutions of varying concentration (2×10^{-5}% to 5×10^{-6}% by weight). The dipole strength was determined for each solution over the frequency range indicated in Table I and averaged to give the reported value.

B. Steady state spectroscopy

Absorbances were measured between 200 and 800 nm in a 1 cm square quartz cuvette using a Perkin Elmer Lambda 40 UV/VIS spectrometer with a scan speed of 240 nm/min and a slit width of 3 nm bandpass. The appropriate solvent was also measured for each material and used for background subtraction. Emission spectra were measured as described in Ref. [29].

C. Time resolved photoluminescence

The excited state lifetimes were measured as follows. The sample was excited with a Tsunami titanium sapphire laser (Spectra-Physics Lasers Inc., Model 3960C-X3BB) tuned to 780 nm, with a pulse length of 73 fs and power output of 7.50 W. A frequency doubling crystal was used to produce a beam of 390 nm. A pulse picker on a 1/10 ratio gave an 8 MHz pulse train with an extinction ratio of approximately 400. The resulting beam was passed through a 390 nm bandpass filter, then used to excite the eumelanin solution contained within a quartz cuvette. The cuvette was measured inside the enclosed cuvette holder (PicoQuant GmbH Rudower Chausse 29, Fluotime 200) with inbuilt detection system (ScienceTech, Inc., Model No. 9030DS). Emission was detected at 475 nm with excitation and emission slits both 2 mm, the iris fully open to give the maximum signal level, and an acquisition time of 1000 s. A blank solution (solvent only) was measured for background subtraction. An instrument response function (IRF) was measured from a Ludox standard scattering solution at the incident wavelength (390 nm) with settings that produced a maximum intensity approximately equal to that of the eumelanin data (excitation and emission slits: 2 mm, acquisition time: 1 s, iris fully closed to prevent detector saturation). Data was deconvolved via an iterative reconvolution process using the multiexponential fluorescence decay fitting software PICOQUANT FLUOFIT.

IV. DENSITY FUNCTIONAL THEORY CALCULATION DETAILS

First principles density functional theory calculations were performed using the Naval Research Laboratory molecular orbital library (NRLMOL) [40–47]. NRLMOL performs massively parallel electronic structure calculation using Gaussian orbital methods. We fully relaxed the geometry with no symmetry constraints using the Perdew, Burke, and Ernzerhof (PBE) [48] exchange correlation functional, which is a generalized gradient approximation (GGA) containing no free parameters.

In the calculations presented in this paper we use the Porezag-Pederson basis sets [49] which have been carefully optimized for the PBE-GGA energy functional using a variational energy criteria. As discussed in Ref. [49], for each atom, the basis sets are optimized with respect to the total number of Gaussian-decay parameters, and with respect to variation of these parameters and the so-called contraction coefficients. There are roughly of triple to quadruple zeta quality. As compared to other Gaussian-basis sets, a key improvement in the PP optimization scheme is that the resulting basis sets satisfy what is now referred to as the $Z^{10/3}$ theorem. This theorem [49] discusses proper scaling of the Gaussian exponents near the nuclei as a function of atomic charge. It has been shown that the resulting PP basis sets exhibit no superposition error and alleviate the need for counterpoise corrections in weakly bound systems. While optimized for PBE-GGA, these basis sets have been tested in HF calculations on polarizabilities as well [50]. The PBE-GGA optimized basis sets deliver HF results in excellent agreement with numerical basis sets (atoms) and polarizabilities of molecules [50]. Basis sets are available upon request.

TABLE II. The transition dipole strengths (D_{DFT}) and frequencies (ν) for tyrosine, DHICA, and fluorescein predicted by DFT. Only the most prominent transitions (those with significant magnitude) in the experimental ranges used in this study are listed. HOMO-LUMO gap for DHICA has been previously reported [65].

	D_{DFT} (Debye^2)	ν (10^{15} Hz)	Transition
Tyrosine	11	0.987	HOMO to LUMO+1
DHICA	49	0.691	HOMO to LUMO
	10	0.743	HOMO−1 to LUMO
Fluorescein	90	0.454	HOMO to LUMO
	9.2	0.500	HOMO−1 to LUMO

Minimum energy structures were calculated for DHICA, tyrosine and fluorescein (chemical structures shown in Fig. 2). We then calculated the strength of each absorption line as the sum over all states of both levels [51] (recall $\mu_{ij} = e\langle j|\vec{r}|i\rangle$)

$$S_{ij} = S_{ji} = \sum_{ij} \mu_{ij}\mu_{ij}. \tag{8}$$

This quantity can be related to the radiative rate A (the Einstein coefficient) via

$$A_{ji}g_j = \frac{64\pi^4\nu^3}{3hc^3}S_{ji} = \frac{2.02\times 10^{18}}{\lambda'^3}S'_{ji}, \tag{9}$$

where no summation over repeated indicies is implied. In the final expression λ' is measured in Å and S'_{ji} is in atomic units [51]. The degeneracy g_j is treated explicitly by NRLMOL. The radiative rate A can be related to the dipole strength via Eq. (5) to give the following expression for the dipole strength:

$$D_{ij} = 6.438S'_{ij}, \tag{10}$$

where D is in D^2 and S' is in atomic units. The dipole strengths of all transitions with energies in the experimental frequency ranges (see Table I) were summed to give the dipole strength values given in Table II.

V. RESULTS AND DISCUSSION

A. Extinction coefficients

Figure 3 compares the measured extinction coefficients for tyrosine, eumelanin, fluorescein, and DHICA as determined experimentally according to Eq. (1). The extinction coefficients for all compounds are in good agreement with literature values [8,52–54], both qualitatively and quantitatively. The extinction coefficient of eumelanin is reported here per monomer, where the molar weight of a monomer is taken to be the average molar weight of DHI and DHICA (171 g mol^{-1}), since we assume that our sample consists of an even mixture of these monomers [55–57]. For such a macromolecule, this is the most meaningful way to express the extinction coefficient. Note the broadband shape of the eumelanin spectrum compared with the more typical peaked

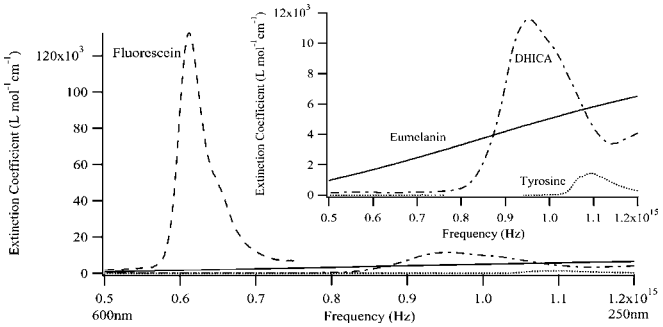

FIG. 3. The extinction coefficients of synthetic eumelanin (solid), DHICA (dot-dash), tyrosine (dotted), and fluorescein (dashed). The inset shows DHICA, eumelanin, and tyrosine data with a different vertical scale (not visible on full plot due to the order of magnitude greater extinction coefficient of fluorescein compared to the other samples). For eumelanin, the extinction coefficient is expressed per monomer. Note the unusual broadband shape of the eumelanin spectrum as compared with the peaked spectra of the other organic molecules. These spectra are in qualitative and quantitative agreement with those in literature [8,52–54]. The much greater magnitude of the fluorescein extinction coefficient is reflected in its much larger dipole strength (see Table I).

spectra of the other organic chromophores. Knowing that our measured extinction coefficients are in good agreement with previously published values, we can now determine other parameters from this data with confidence.

B. Transition dipole strengths

Dipole strengths, transition dipole moments, and oscillator strengths for each of these compounds were determined from the measured extinction coefficients according to Eqs. (2)–(4), and are shown in Table I. For eumelanin the average molar weight is taken to be the average number of monomers per oligomer (N), multiplied by the average molar weight of the two forms of eumelanin precursor (171 g mol^{-1}). The extinction coefficient and other parameters discussed in Sec. II then become functions of N, and are expressed as such in Tables I and IV. Values in brackets for tyrosine and fluorescein are from Ref. [54] for comparison. Our results are consistent with literature values; discrepancies can be attributed to differences in solvent (which may affect the dipole strength via second order effects). Refer to the discussion in the theory section for more details.

Note that the parameters shown in Table I are usually calculated over a particular single transition, whereas for eumelanin this is unachievable due to the broadband shape of the absorption spectrum. For typical compounds, the extinction coefficient is small outside of a clear peak, and hence increasing the integration range will not greatly affect the estimate of the dipole strength. For eumelanin, however, there is no clear peak, so increasing the integration range (particularly towards the UV) will increase the estimate of the dipole strength. We have chosen the relevant integration range 250 to 800 nm, which gives an order of magnitude estimate of the dipole strength in a critical range from a functional perspective. DHICA was integrated over the same range as eumelanin so that a direct comparison is possible. Tyrosine and fluorescein exhibit clear peaks, so that the integration range is not particularly important.

Transition dipole moments and oscillator strengths have also been included in Table I since these are other commonly used measures of the same parameter. Note that if eumelanin forms large polymer structures this would make the number of monomers per oligomer (N) very large, and hence the dipole strength very large. This does *not* mean, however, that the polymerization process enhances the absorption of a solution of eumelanin relative to its precursors, since as the polymerization process occurs the total number of species in the solution decreases. This means that although the dipole strength increases, the concentration decreases in such a way that the optical density of the solution may stay approximately constant.

In summary, the dipole strength per monomer of eumelanin over the UV/ visible range was determined to be approximately 40 D^2 (Table I). This is greater than the dipole strength of tyrosine (1.6 D^2), comparable to that of DHICA (31 D^2), and less than that for fluorescein (140 D^2). These results suggest that eumelanin is neither an exceptionally strong absorber (as one might expect due to its biological role as a photoprotectant), nor exceptionally weak.

C. Transition dipole strengths from density functional theory

First principles quantum chemistry calculations are routinely used as a standard tool for assessing such properties of materials as optical and electrical parameters, electronegativity, hardness, softness, molecular energetics and other properties [58]. Here we use density functional theory (DFT) to assess whether our experimentally determined optical parameters are in agreement with quantum chemical models for these systems. This provides important validation of our experimental results, and a benchmark for further use of DFT in studies of this nature.

The transition dipole strengths and energy gaps (listed as frequencies) of the structurally well characterized molecules examined here were calculated using DFT, and are listed in Table II. More than one transition was predicted to lie within the experimental frequency ranges, most of which had negligible dipole strengths. Hence only those predicted to have substantial magnitudes are listed. The fourth column lists the main transitions that are predicted to make substantial contributions to the dipole strength. Note that for tyrosine the HOMO to LUMO transition has negligible intensity (and hence is not listed), whereas that transition dominates the dipole strengths of DHICA and fluorescein. Similarly, for both DHICA and fluorescein the HOMO−1 to LUMO transition makes the next most intense contribution to the dipole strength, and is located close in energy to the HOMO to LUMO transition. For tyrosine, however, all higher energy transitions with substantial intensity were far removed from the initial peak, occurring at much higher energies and close to the upper bounds of the experimental frequency range. With the known tendency of DFT to underestimate energy gaps (as discussed below), we believe that these higher energy transitions were not related to the experimentally mea-

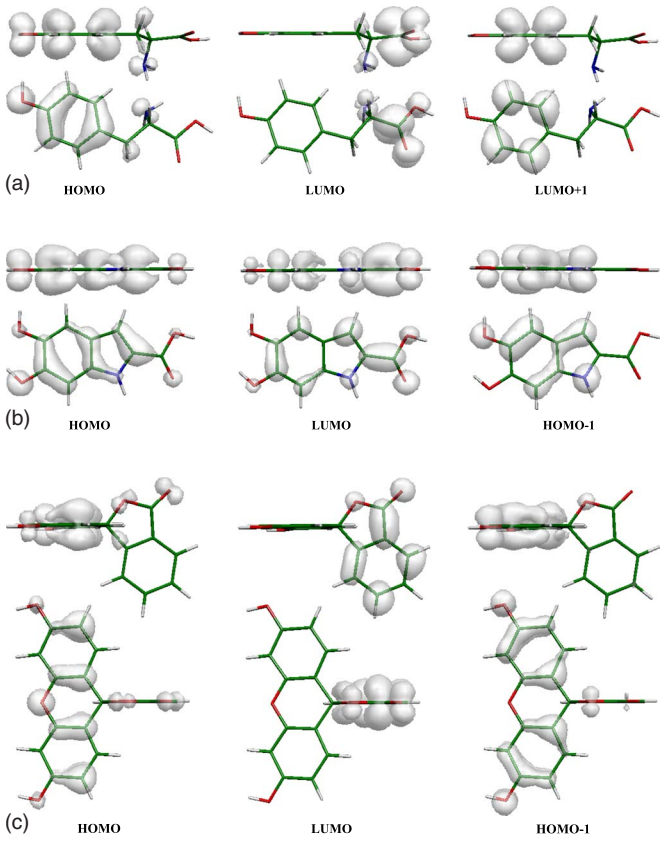

FIG. 4. (Color online) Electron densities of important molecular orbitals as calculated by NRLMOL. The HOMO to LUMO+1 transition is predicted to be that with substantial oscillator strength for tyrosine as shown in Table II; the tyrosine LUMO is also shown for comparison to DHICA and fluorescein. The HOMO to LUMO and HOMO−1 to LUMO transitions are predicted to be those with substantial oscillator strengths for fluorescein and DHICA, as shown in Table II. Red: oxygen, blue: nitrogen, green: carbon, white: hydrogen.

sured extinction coefficient peaks, and hence have not been considered in this analysis. It is curious that tyrosine differs qualitatively from DHICA and fluorescein; we believe this is an interesting topic for further investigation.

The electron densities calculated by DFT of the important molecular orbitals for these molecules are shown in Fig. 4. For DHICA and fluorescein the HOMO to LUMO and HOMO−1 to LUMO transitions are those predicted to make significant contributions to the dipole strength. It is clear that the electron densities of each of these three important molecular orbitals for DHICA and fluorescein have nodes in the plane of the molecule, and therefore can be attributed to π orbitals. This suggests that both of these transitions are π-π^*, as would be expected for transitions at these energies for organic molecules of this type. It is interesting to note that while DHICA has a relatively even electron distribution in all states shown, fluorescein shows a significant movement of electron density from one part of the molecule to the other in both the HOMO to LUMO and HOMO−1 to LUMO transitions.

The electron densities for tyrosine are more difficult to interpret because this molecule has a nonplanar section. All three molecular orbitals appear to have π character, however, indicating that the HOMO to LUMO+1 transition (the only transition of experimental relevance with significant intensity) is also a π-π^* transition. Interestingly, both the HOMO and LUMO+1 appear to have the electron density localized largely on the aromatic group, whereas the LUMO (not involved in any significant transitions) has electron density localized on the nonaromatic tail group.

Transition dipole strengths and frequencies for each of these molecules calculated from DFT are shown in Table III, compared with those determined from the experimentally measured extinction coefficient for these molecules. It can be seen that PBE-DFT consistently underestimates the energy gap by ~10–30 %, as is typically observed [59]. Due to broadening of experimental data we must choose an integration range to achieve a quantitative comparison of these DFT predicted dipole strengths to experiment. Since there were multiple transitions predicted for the energy ranges used experimentally, the dipole strengths of all transitions in the range for DHICA and fluorescein were summed to give the value for comparison to experiment, as shown in Table III. For tyrosine, the positioning of the DFT predicted peaks suggested that only the HOMO to LUMO+1 transition should be compared to the experimental data (as discussed above).

We emphasize that DFT is a theory of the ground state, however it can reproduce trends in excited state behavior (including transition energies and dipole strengths) [60,61]. It is clear from Table III that although DFT does not give

TABLE III. Dipole strengths D calculated using density functional theory (in vacuum D_{DFT}) compared with experiment (in solution D_{exp}). $\Delta\nu_{\mathrm{exp}}$ are the frequency ranges over which the integrations of the experimental data were performed to determine the dipole strength. These ranges were also used to sum the DFT peaks for DHICA and fluorescein to obtain the values listed, whereas for tyrosine only the lowest energy DFT peak was considered to contribute, since it appears that the higher energy peaks in the DFT are not relevant to the experimental spectrum. Essential trends in the dipole strength are reproduced by the DFT results. The frequency where the main peak occurs experimentally (ν_{av}, experimental) can be compared to the frequencies for the main DFT predicted transitions (ν_{av}, DFT); as has been previously observed DFT consistently underestimates the magnitude of the energy gap but reproduces trends correctly [59].

	Experiment			DFT		
	D_{exp} (Debye^2)	ν_{av} (10^{15} Hz)	$\Delta\nu_{\mathrm{exp}}$ (10^{15} Hz)	D_{DFT} (Debye^2)	ν_{av} (10^{15} Hz)	Transitions used for D_{DFT}
Tyrosine	1.6	1.09	0.38 to 1.2	11	0.987	ν=0.987, HOMO to LUMO+1
DHICA	31	0.949	0.50 to 1.2	66	0.691	Total in experimental range
Fluorescein	140	0.611	0.44 to 0.75	112	0.454	Total in experimental range

TABLE IV. Radiative rates (A) and lifetimes (τ) calculated from emission and absorption spectra of eumelanin, tyrosine, and fluorescein. λ_{ex} is the excitation wavelength and Φ is the radiative quantum yield. The extinction coefficient and fluorescence spectra for tyrosine used for these calculations are from Ref. [54]. The directly measured lifetimes agree to within an order of magnitude with those determined from the extinction coefficients, which is good considering that many parameters (such as the absorption coefficient, radiative quantum yield, and the solution concentration), each with their own uncertainties, enter into determining this value. Also, we have used a first order theory that does not take higher order effects into account. Therefore, we are satisfied with this level of agreement with literature.

		A (ns^{-1})		Φ	τ	
	λ_{ex} (nm)	(these results)	(literature)	(literature)	(these results)	(literature)
Eumelanin	380	$0.13N$		$(6.42\pm0.3)\times10^{-4}$ [29]	$4.9N^{-1}$ ps	$\leqslant$85 ps [29]
Fluorescein	490	0.38	0.221 [32]	0.92 ± 0.02 [32]	2.4 ns	4.2 ns [32]
Tyrosine	274	0.0082		0.13 [52]	16 ns	3.4 ns [52,67]

strong quantitative agreement with the dipole strengths measured experimentally (particularly for tyrosine), it does reproduce the experimentally observed trends, giving the smallest dipole strength for tyrosine, and the largest for fluorescein. This shows that DFT is an appropriate tool for qualitatively modeling eumelanin and similar systems. The ability of DFT to reproduce the trends in the dipole strength also lends weight to our experimental results.

It is somewhat curious that better quantitative agreement is not observed between DFT results and experiment. As exemplified in Ref. [50] and references within that paper, it is well accepted that DFT delivers very accurate molecular polarizabilities (certainly better than 10%). The polarizability of a molecule depends quadratically upon the same dipole matrix elements that appear in the expression for absorptivity [Eq. (9)] which also depends quadratically upon these elements. Therefore deviation between theoretical and experimental trends in Table III, particularly tyrosine, must be viewed as inexplicably large in comparison to 10–30 % deviations in energy gaps observed for these molecules and ~5% deviations in screened polarizabilities.

A number of theoretical techniques could provide more accurate values of the dipole strength. Time-dependent DFT (TDDFT) has been shown to be effective for predicting excited state properties such as transition energies and optical absorption spectra [62]. Further, Yabana and Bertsch have shown that TDDFT reproduces dipole strengths of π-π^* transitions for conjugated carbon molecules with a typical accuracy of ~20% [63]. The fact that TDDFT only reproduces dipole strengths in π-π^* transitions for conjugated carbon molecules to 20% is indeed interesting given that a large body of results shows that DFT-based static polarizabilities lead to better agreement than this. It is also interesting to note in this context that Olsen *et al.* [64] have recently calculated the oscillator strengths for several oxidized forms of DHICA using state averaged complete active space calculations [SA3-CAS(4,3)] and multireference perturbation theory (MRPT2). These methods should be expected to provide higher accuracy than either DFT or TDDFT. However, Olsen *et al.* find oscillator strengths at least as large as the DFT results reported above for DHICA. This suggests that the disagreement between theory and experiment may not be solely due to the limitations of DFT. Understanding the origin of this deviation should be a future effort.

D. Prediction of radiative rates and lifetimes

Radiative rates and lifetimes were determined for eumelanin, tyrosine and fluorescein using previously measured emission spectra, and quantum yield values [29,32,54] in addition to the extinction coefficients reported here, as outlined in the theory section. These are shown in Table IV. The radiative quantum yield of eumelanin is known to vary with excitation wavelength [29] (this is an unusual property for an organic chromophore [66]). For calculations here, the value at $\lambda_{ex}=380$ nm has been used (where λ_{ex} is the excitation wavelength). A and τ for fluorescein agree well with literature values which lends credibility to our values for eumelanin. Similarly, the lifetime predicted for tyrosine is consistent with the reported literature value.

For a further comparison of the parameters determined from the extinction coefficient, the excited state lifetime of eumelanin was measured directly. The decay was found to be multiexponential, with lifetimes and relative amplitudes as shown in Table V. The predominant lifetime is the shortest: 85 ps. This is of the order of the instrument response, such that the actual predominant lifetime may be much shorter. These results are consistent with those reported by Forest [68] (predominant radiative lifetime of 59 ps at 420 nm). Note that this value is also likely to be an overestimate of the true radiative lifetime of eumelanin. Hence, we conclude that the excited state lifetime of eumelanin determined from the absorption and emission spectra is consistent with the di-

TABLE V. Multiexponential fit parameters for the experimentally measured photoluminescence excitation decay of eumelanin. The predominant excited state lifetime (85 ps) is relatively short, and may be shorter (this time is of the order of the instrument response function). The consistency between these measured lifetimes and that determined from the absorption and emission spectra is consistent with the broadband absorption spectrum being electronic in origin.

Lifetime (ns)	Relative amplitude
$\leqslant$0.085	51%
0.93	27%
3.5	17%
9.8	5.2%

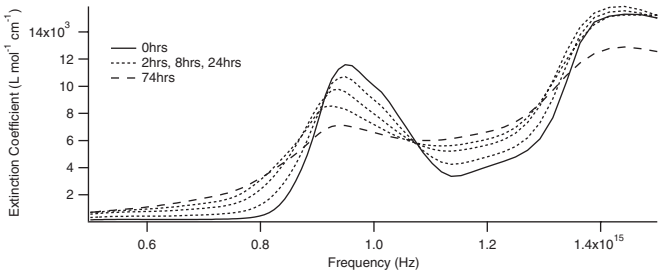

FIG. 5. The extinction coefficient per monomer of DHICA as it undergoes oxidative polymerization to form eumelanin. The initially peaked DHICA spectrum gradually shifts towards the broadband eumelanin spectrum, but does not change substantially in integration area. Dipole strengths determined from this data are shown in Fig. 6.

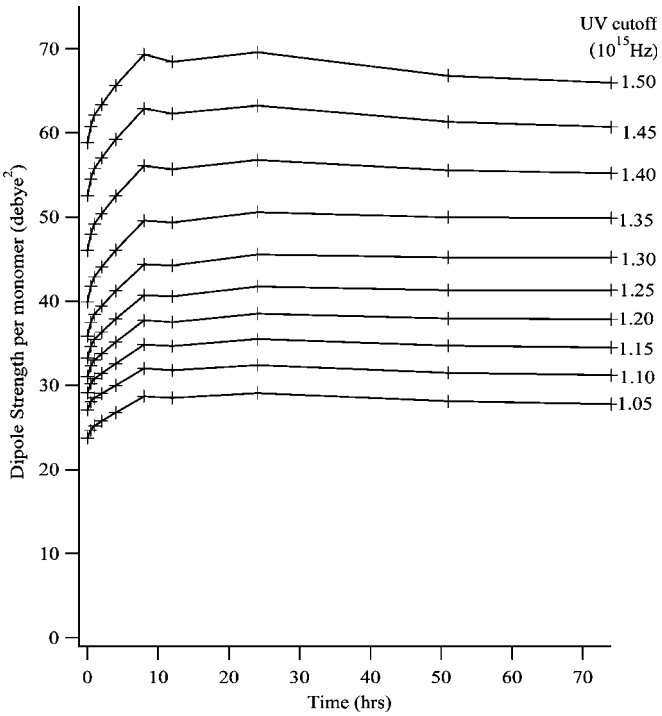

FIG. 6. The dipole strength per monomer of DHICA over time, as it reacts to form eumelanin, determined using different UV cutoff frequencies. The variation between the curves indicates that the absolute value of the dipole strength at each time point is only accurate to within an order of magnitude. The overall increase in dipole strength is, however, more robust, showing that eumelanin exhibits between 12 and 26 % hyperchromism (increase in dipole strength with polymerization).

rectly measured lifetime. This agreement indicates that the absorption spectrum of eumelanin is genuinely electronic in origin, and not a result of scattering or some other nonelectronic phenomenon (as has been suggested due to the broadband shape of the eumelanin absorption spectrum [16]). This has since been shown to be the case [69]; the optical density of a eumelanin solution is predominantly due to electronic transitions and not a scattering phenomenon. The successful prediction of the lifetimes and radiative rates for eumelanin and the other compounds studied here indicates that the dipole strengths determined from this same data are reliable.

E. Time evolution of DHICA into eumelanin

So far we have considered the equilibrium properties of eumelanin and DHICA. It is now instructive to consider how these spectroscopic properties change in the reaction process as DHICA evolves to form eumelanin. DHICA was allowed to react and the absorbance monitored at intervals. The extinction coefficient as it evolves over time is shown in Fig. 5. The shape of the DHICA spectrum (measured at the initial time) is in good agreement with published spectra [38,70], and as it reacts it shifts towards the eumelanin spectrum (both in shape and magnitude), as would be expected. Note that the extinction coefficient is plotted per monomer, since this is a more meaningful parameter for a macromolecule than the absolute extinction coefficient.

The dipole strength per monomer was determined at each time point, and is plotted in Fig. 6 for different choices of UV cutoff frequency. Note that although the absolute magnitude of the eumelanin dipole strength is affected by the choice of integration range, the relative change in dipole strength over the course of the reaction is more robust. The dipole strength per monomer increases by approximately 20% over the course of the reaction (the increase is between 12 and 26 % for the UV cutoff frequencies we have considered). The dipole strength tends towards the value measured for eumelanin, as would be expected (when the same UV cutoff frequency is used for both).

This data indicates that eumelanin exhibits hyperchromism; the reaction process enhances absorption such that after the reaction the dipole strength of an oligomer is greater than the sum of the dipole strengths of the constituent monomers (for a discussion of hypochromism in biological molecules see Ref. [71]). The observed hyperchromism of eumelanin is interesting; biopolymers often exhibit hypochromism (decrease in UV and visible dipole strength per monomer upon polymerization) of a similar magnitude to the hyperchromism we observe for eumelanin (5–10 % for polystyrene [72,73], 19–25 % for poly(N-vinylcarbazole) [74], and 40% for DNA [71]). The hypochromism in these molecules is thought to be related to the formation of π-stacking interactions, which reduce the oscillator strength due to the parallel and adjacent arrangement of transition dipoles of the neighboring molecules [75–78]. Hyperchromism, on the other hand, can occur when the dipoles of neighboring molecules are arranged along the same axis and one behind the other. The hyperchromism observed for eumelanin might therefore be due to the edgewise association of DHICA molecules, forming planar oligomers. A slight hypochromism is also observed at later times, which may suggest subsequent π stacking of planar oligomers. We wish to emphasize, however, that the magnitude of the observed hyperchromism (and especially the later hypochromism) is very small, and is of the order of the uncertainty due to the choice of UV cutoff frequency. We therefore caution that these results should not be over analyzed without first measuring the extinction coefficient further into the UV.

Eumelanin's hyperchromism could be related to its role as a biological photoprotectant (an increase in absorption strength upon polymerization enhances its ability to shield from incident photons). The fact that the magnitude of the hyperchromism is small, however, indicates that it is likely to be biologically less important than the evolution from a peaked spectrum to a more broadband absorption spectrum. Most significantly, these results are consistent with the chemical disorder structural model for eumelanin [9]. In this model, the broadband absorption spectrum of eumelanin is produced by the summation of the (peaked) spectra of many distinct chemical species. These species are suggested to be small oligomers of DHI and DHICA (Fig. 2) which would be expected to have dipole strengths per monomer similar to those of the monomer species (being similar in size). Since we observe only a small increase in the dipole strength per monomer over the course of the reaction, we conclude that these results are consistent with this model.

VI. CONCLUSIONS

We have shown that the dipole strength of eumelanin is not exceptional compared to other biologically relevant molecules. The dark coloring and photoprotection in the skin and hair of humans and other species must therefore be the result of a concentration effect. Our results also suggest that the highly unusual broadband absorption spectrum of eumelanin is electronic in origin, and not caused by scattering or other nonelectronic processes, as has been suggested. In addition, we found that the dipole strength per monomer of eumelanin increases by approximately 20% as it forms, indicating that eumelanin exhibits hyperchromism. Most significantly, the small magnitude of this hyperchromism is consistent with the currently favoured secondary structural model of eumelanin (the chemical disorder model). It also suggests that the most important role of the reaction that forms eumelanin is to produce a broadband absorption spectrum, rather than an increased dipole strength. The resulting broadband absorption spectrum of eumelanin makes it capable of acting as an optical filter, protecting biological tissue from optical damage.

ACKNOWLEDGMENTS

We thank Jacques Bothma and Seth Olsen for helpful discussions. Work at the University of Queensland and the Naval Research Laboratory was partly funded by the Australian Research Council. Calculations were performed on the Australian Partnership for Advanced Computing (APAC) National Facility under a grant from the Merit Allocation Scheme.

[1] G. Prota, *Melanins and Melanogenesis* (Academic Press, San Diego, 1992).
[2] A. Vitkin, J. Woolsey, B. C. Wilson, and R. R. Anderson, Photochem. Photobiol. **59**, 455 (1994).
[3] N. Kollias, R. M. Sayer, L. Zeise, and M. R. Chedekel, J. Photochem. Photobiol., B **9**, 135 (1991).
[4] M. B. Youdim, D. Ben-Shachar, and P. Riederer, Acta Neurol. Scand. Suppl. **126**, 47 (1989).
[5] D. M. Mann and P. O. Yates, Mech. Ageing Dev. **21**, 193 (1983).
[6] H. Z. Hill, W. Li, P. Xin, and D. L. Mitchell, Pigment Cell Res. **10**, 158 (1997).
[7] P. Meredith and T. Sarna, Pigment Cell Res. **19**, 572 (2006).
[8] T. Sarna and H. M. Swartz, *The Physical Properties of Melanins* (Oxford University Press, New York, 1987).
[9] P. Meredith, B. J. Powell, J. Riesz, S. Nighswander-Rempel, M. R. Pederson, and E. Moore, Soft Matter **2**, 37 (2006).
[10] R. D. Vecchio and N. V. Blough, Environ. Sci. Technol. **38**, 3885 (2004).
[11] R. G. Zepp and P. F. Schlorzhauer, Chemosphere **10**, 479 (1981).
[12] A. Bricaud, A. Morel, and L. Prieur, Limnol. Oceanogr. **26**, 43 (1981).
[13] N. V. Blough and R. D. Vecchio, *Biogeochemistry of Marine Dissolved Organic Matter* (Academic Press, San Diego, 2002).
[14] S. A. Green and N. V. Blough, Limnol. Oceanogr. **39**, 1903 (1994).
[15] N. V. Blough, O. C. Zafiriou, and J. Bonilla, J. Geophys. Res. **98**, 2271 (1993).
[16] M. Wolbarsht, A. Walsh, and G. George, Appl. Opt. **20**, 2184 (1981).
[17] J. Riesz, J. Gilmore, and P. Meredith, Spectrochim. Acta, Part A **61**, 2153 (2005).
[18] T. Strzelecka, Physiol. Chem. Phys. **14**, 219 (1982).
[19] J. E. McGuiness, Science **177**, 896 (1972).
[20] J. E. McGuiness, Jpn. Circ. J. **39**, 677 (1973).
[21] A. Pullman and B. Pullman, Biochim. Biophys. Acta **54**, 384 (1961).
[22] P. R. Crippa, V. Cristofoletti, and N. Romeo, Biochim. Biophys. Acta **583**, 164 (1978).
[23] H. C. Longuet-Higgins, Arch. Biochem. Biophys. **86**, 231 (1960).
[24] J. E. McGuinness, P. Corry, and P. M. Proctor, Science **183**, 853 (1974).
[25] A. M. Potts and P. C. Au, Agressologie **9**, 225 (1968).
[26] E. M. Trukhan, N. F. Perevoschikoff, and A. M. Ostrovski, Biofizika **15**, 1052 (1970).
[27] E. M. Trukhan, V. N. Deryabkin, and A. M. Ostrovski, Biofizika **18**, 392 (1973).
[28] M. L. Tran, B. J. Powell, and P. Meredith, Biophys. J. **90**, 743 (2006).
[29] P. Meredith and J. Riesz, Photochem. Photobiol. **79**, 211 (2004).
[30] R. S. Knox, Photochem. Photobiol. **77**, 492 (2003).
[31] P. W. Atkins, *Molecular Quantum Mechanics*, 3rd ed. (Oxford University Press, New York, 1996).
[32] D. Magde, R. Wong, and P. G. Seybold, Photochem. Photobiol. **75**, 327 (2002).

[33] R. S. Knox (unpublished).
[34] A. Bartczak, A. Dudkowiak, and D. Frackowiak, Photochem. Photobiol. **78**, 525528 (2003).
[35] L. Onsager, J. Am. Chem. Soc. **58**, 1486 (1936).
[36] G. D. Mahan, *Many-Particle Physics*, 2nd ed. (Plenum Press, New York, 1990).
[37] C. Bottcher, *Theory of Electric Polarization* (Elsevier, Amsterdam, 1973), Vol. 1.
[38] X. Zhang, C. Erb, J. Flammer, and W. M. Nau, Photochem. Photobiol. **71**, 524 (2000).
[39] A. Tamulis, J. Tamuliene, M. L. Balevicius, Z. Rinkevicius, and V. Tamulis, Struct. Chem. **14**, 643 (2003).
[40] M. Pederson, D. Porezag, J. Kortus, and D. Patton, Phys. Status Solidi B **217**, 197 (2000).
[41] M. R. Pederson and K. A. Jackson, Phys. Rev. B **41**, 7453 (1990).
[42] K. A. Jackson and M. R. Pederson, Phys. Rev. B **42**, 3276 (1990).
[43] M. R. Pederson and K. A. Jackson, Phys. Rev. B **43**, 7312 (1991).
[44] A. A. Quong, M. R. Pederson, and J. L. Feldman, Solid State Commun. **87**, 535 (1993).
[45] D. V. Porezag and M. R. Pederson, Phys. Rev. B **54**, 7830 (1996).
[46] D. V. Porezag, Ph.D. thesis, Technische Universitait, Chemnitz, 1997.
[47] A. Briley, M. R. Pederson, K. A. Jackson, D. C. Patton, and D. V. Porezag, Phys. Rev. B **58**, 1786 (1998).
[48] J. P. Perdew, K. Burke, and M. Ernzerhof, Phys. Rev. Lett. **77**, 3865 (1996).
[49] D. Porezag and M. R. Pederson, Phys. Rev. A **60**, 2840 (1999).
[50] M. Pederson, T. Baruah, P. Allen, and C. Schmidt, J. Chem. Theory Comput. **1**, 590 (2005).
[51] H. G. Kuhn, *Atomic Spectra*, 2nd ed. (Academic Press, New York, 1969), p. 337.
[52] G. D. Fasman, *Proteins*, 3rd ed. (CRC Press, Cleveland, Ohio, 1976), Vol. 1, pp. 183–203.
[53] P. C. DeRose and G. W. Kramer, J. Lumin. **113**, 314 (2005).
[54] P. C. DeRose and G. W. Kramer, Photochem. Photobiol. **168**, 141 (1998).
[55] S. Ito, Biochim. Biophys. Acta **883**, 155 (1986).
[56] K. Wakamatsu and S. Ito, Pigment Cell Res. **15**, 174 (2002).
[57] A. Pezzella, D. Vogna, and G. Prota, Tetrahedron **58**, 3681 (2002).
[58] A. Nagy, Phys. Rep. **298**, 2 (1998).
[59] R. O. Jones and O. Gunnarsson, Rev. Mod. Phys. **61**, 689 (1989).
[60] E. K. U. Gross, J. F. Dobson, and M. Petersilka, *Density Functional Theory* (Springer, Berlin, 1996).
[61] M. Petersilka, U. J. Gossmann, and E. K. U. Gross, Phys. Rev. Lett. **76**, 1212 (1996).
[62] J. R. Chelikowsky, L. Kronik, and I. Vasiliev, J. Phys.: Condens. Matter **15**, R1517 (2003).
[63] K. Yabana and G. F. Bertsch, Int. J. Quantum Chem. **75**, 55 (1999).
[64] S. Olsen, J. Riesz, I. Mahadevan, A. Coutts, J. P. Bothma, B. J. Powell, R. H. McKenzie, S. C. Smith, and P. Meredith, J. Am. Chem. Soc. **129**, 6672 (2007).
[65] B. J. Powell, Chem. Phys. Lett. **204**, 111 (2005).
[66] Jobin Yvon Horiba and Stanmore, *A Guide to Recording Fluorescence Quantum Yields*, http://www.jobinyvon.co.uk, 2007.
[67] K. Guzow, R. Ganzynkowicz, A. Rzeska, J. Mrozek, M. Szabelski, J. Karolczak, A. Liwo, and W. Wiczk, J. Phys. Chem. B **108**, 3879 (2004).
[68] S. E. Forest, W. C. Lam, D. P. Millar, J. B. Nofsinger, and J. D. Simon, J. Phys. Chem. B **104**, 811 (2000).
[69] J. Riesz, J. Gilmore, and P. Meredith, Biophys. J. **90**, 1 (2006).
[70] W. H. Koch and M. R. Chedekel, Photochem. Photobiol. **46**, 229 (1987).
[71] K. E. van Holde, W. C. Johnson, and P. S. Ho, *Principles of Physical Biochemistry* (Prentice-Hall, Englewood Cliffs, NJ, 1998).
[72] M. T. Vala and S. A. Rice, J. Chem. Phys. **39**, 2348 (1963).
[73] J. Kowal and D. Jamroz, Makromol. Chem. **192**, 461 (1991).
[74] J. Kowal, Macromol. Chem. Phys. **196**, 1195 (1995).
[75] I. Tinoco, J. Am. Chem. Soc. **82**, 4785 (1960).
[76] C. R. Cantor and P. R. Schimmel, *Biophysical Chemistry Part II: Techniques for the Study of Biological Structure and Function* (Freeman, San Francisco, CA, 1980), p. 399.
[77] H. Neuhacher and W. Lohmann, in *Biophysics*, edited by W. Hoppe, W. Lohmann, H. Markl, and H. Ziegler (Springer, Berlin, 1983), Chap. 3.2.5, p. 106.
[78] F. Peral and E. Gallego, Spectrochim. Acta, Part A **56**, 2149 (2000).